Simulation and Optimization of the Continuous Tower Process for Styrene Polymerization

Shrikant A. Bhat, Rahul Sharma, Santosh K. Gupta

Department of Chemical Engineering, Indian Institute of Technology, Kanpur 208016, India

Received 2 June 2003; accepted 7 April 2004
DOI 10.1002/app.20941
Published online in Wiley InterScience (www.interscience.wiley.com).

ABSTRACT: The continuous tower process, a popular industrial process for the manufacture of polystyrene, was simulated and optimized. A kinetic model for the thermal polymerization of styrene, which takes into account the Trommsdorff effect and the volume change accompanying the reaction, was developed. This was used to formulate model equations for the continuous flow stirred tank reactor (CSTR) and plug flow reactor (several sections) in the tower process. The model can predict monomer conversion, number- and weight-average molecular weights, polydispersity index (PDI), and temperature at various locations in the unit, under specified operating conditions. Multiobjective optimization of this process was also carried out, for which an adaptation of a genetic algorithm (GA) was used. The two objectives were maximization of the final monomer conversion and minimization of the PDI of the product. The conversion in the CSTR was constrained to lie within a desired range, and polymer having a specified value of the number-average molecular weight was to be produced. The optimal solution was a unique point (no Pareto sets were obtained). The optimal solutions indicated that the tower process is operated under near-optimal conditions. © 2004 Wiley Periodicals, Inc. J Appl Polym Sci 94: 775–788, 2004

Key words: genetic algorithm (GA); modeling; reactive processing; polystyrene; tower process

INTRODUCTION

The thermal polymerization of styrene has interested researchers for over six decades. Flory[1] pioneered studies in this field by suggesting a mechanism for this reaction, as early as in 1937, based on an initiation step that involved the combination of two styrene molecules to produce a diradical. However, his mechanism did not gather much support because subsequent studies by Haward,[2] Zimm and Bragg,[3] Russell and Tobolosky,[4] and Overberger and Lapkin[5] indicated that diradicals cyclize too rapidly to initiate the polymerization of styrene. Obviously, there was a need for a better mechanism: this was provided by Mayo,[6] who suggested that the first step in the kinetic mechanism is the Diels–Alder dimerization of styrene to form 1,2,3,9-tetrahydronaphthalene (AH in Table I), which subsequently reacts with a third styrene molecule to produce a styryl (A) and a 1-phenyltetralyl ($PhCHCH_3$) radical. Both these radicals can initiate polymerization (all the reactions are not shown in Table I). Propagation occurs in the usual manner and termination occurs both by combination and chain transfer to monomer. The greatest success of this mechanism lay in its ability to account for the observed order of 5/2 of the overall rate of polymerization with respect to the styrene concentration. Hui and Hamielec[7] carried out an experimental study of this reaction and proposed a kinetic model that satisfactorily predicted the observed conversion, average molecular weights, and the molecular weight distribution in an isothermal batch reactor. They also incorporated the Trommsdorff effect[8] in their model. The applicability of their model is, however, constrained by the range (100–200°C) of temperature selected for experimentation.

Although the model can easily be extrapolated for temperatures below 100°C, the presence of a logarithmic term in the rate constant k_{fm} for chain transfer to monomer (which blows up as soon as the temperature exceeds 200°C) does not allow extrapolation beyond 200°C. This, in fact, is not a severe restriction because industrial processes for the production of polystyrene usually limit the reactor temperatures to below 200°C, to ensure that the polymer has a molecular weight of commercial value and is low in oligomer content. Wallis et al.[9] analyzed the bulk polymerization of styrene by AIBN initiator in a tubular reactor. They used both the plug flow model as well as a model incorporating diffusion terms for simulating the tubular reactor and concluded that use of the latter did not lead to any significant improvements in the results and that the simpler plug flow model is adequate to

Correspondence to: S. Gupta (skgupta@iitk.ac.in).
Contract grant sponsor: Department of Science and Technology, Government of India, New Delhi; contract grant number: III-5(13)/2001-ET.

TABLE I
Kinetic Mechanism for the Thermal Polymerization of Styrene[7]

Initiation	$S + S \rightleftarrows AH$
	$S + AH \rightarrow PhCHCH_3 + A$
	$S + AH \rightarrow \text{Trimer}$
	$A + S \rightarrow R_1$
	$S + S \rightarrow R_1$
Propagation	$R_r + S \xrightarrow{k_p} R_{r+1}$
Termination	$R_r + R_s \xrightarrow{k_t} P_{r+s}$
	$R_r + S \xrightarrow{k_{fm}} P_r + R_1$

describe the polymerization. Their results, although in close agreement with experimental data, cannot describe the industrial bulk polymerization of styrene because they fall in a very narrow range (10–35%) of monomer conversion.

Tadmor and Biesenberger[10] presented analytical results for monomer conversion and molecular weight distribution in continuous flow stirred tank reactors (CSTRs) for polymerizations involving chain addition of simple monomers in the presence of the termination step. Gao et al.[11] reviewed the commonly used optimization policies for the manufacture of polystyrene. These workers suggested that an optimal temperature profile/history, along with the selective addition of mono- or bifunctional initiators, can decrease the batch time while still maintaining the desired properties of the polymer produced. Husain and Hamielec[12] conducted the most extensive study on the thermal polymerization of styrene in a tubular reactor. They studied the effect of the tube diameter and the wall temperature on the monomer conversion, the molecular weight distribution, and the maximum temperature attained in the reactor. They also suggested commercially viable combinations of CSTRs and tubular reactors for the industrial production of polystyrene. However, it is unlikely that any of these combinations can be implemented in industry because they are either incapable of attaining high monomer conversions, or the maximum temperature in these reactors rises to unacceptably high levels. However (to the best of our knowledge), this[12] is the only study on the industrial-scale thermal polymerization of styrene in the open literature. The present study is an attempt to continue work along this direction by studying a popular, although relatively old, industrial process for the production of polystyrene: the continuous tower process.

Several technologies have been patented[13–18] for the commercial production of polystyrene. Among these, the continuous tower process, patented by I. G. Farbenindustrie[13,14] in 1936, has been quite popular: it is one of the oldest industrial processes used for the thermal polymerization of styrene. The processes subsequently developed by Union Carbide[15] and Dow[16–18] are modifications of this process. Details of the continuous tower process can be found elsewhere.[13,14,18–21] In this process (see Fig. 1), thermal polymerization is carried out in two parallel CSTRs, followed by a single tubular reactor with temperature programming. Pure styrene is fed to each of the CSTRs at a rate of $M_0^*/2$ mol s^{-1}. Each CSTR has a volume V_c and is maintained at a constant temperature T_c, by the circulation of water through internal coils. The outlet of the two CSTRs is combined and fed to the tubular reactor. The latter is composed of six equal sections, the wall temperature (of the external jacket and the internal cooling coil) of the ith section being maintained at temperature T_{wi} (Fig. 1). Table II (second column) provides the range of values used industrially[20,21] for T_c and T_{wi}. The product from the last section is heated to about 200°C and fed to devolatilizing extruders to remove the unreacted monomer (which is recycled).

In this study, we first model the continuous tower process and then optimize it to see whether the temperature profiles used industrially are, indeed, optimal. The elitist nondominated sorting genetic algorithm (NSGA-II), developed by Deb et al.,[22,23] was used to optimize the tower process. In this technique, several chromosomes (solutions) are generated, and the population of chromosomes evolves over the generations to give, finally, the optimal solutions, exploiting the Darwinian principle of survival of the fittest. Further details of this algorithm can be found in Deb,[22] Deb et al.,[23] and Bhaskar et al.,[24] and are not provided here. The algorithm can solve problems involving both single and multiple objectives and has been used extensively in the last decade to study a variety of problems in chemical and polymerization engineering.[24] These include, for example, the fluidized-bed catalytic cracking unit,[25] steam reformer,[26,27] crude distillation unit,[28] batch free-radical polymerization,[29] semibatch copolymerization reactors,[30] wastewater treatment,[31] hydrogen plant,[32] simulated countercurrent moving bed chromatographic reactor,[33] and reactive simulated moving bed reactor.[34] Kasat et al.[35] and Nandasana et al.[36] recently updated the earlier review of Bhaskar et al.[24] on single and multiobjective optimization studies in chemical engineering, using GA and its adaptations.

FORMULATION

Modeling

The kinetic mechanism of thermal polymerization used in this work, presented in Table I, is the same as that used by Hui and Hamielec.[7] Mass balance and moment equations, describing the two reactors (a se-

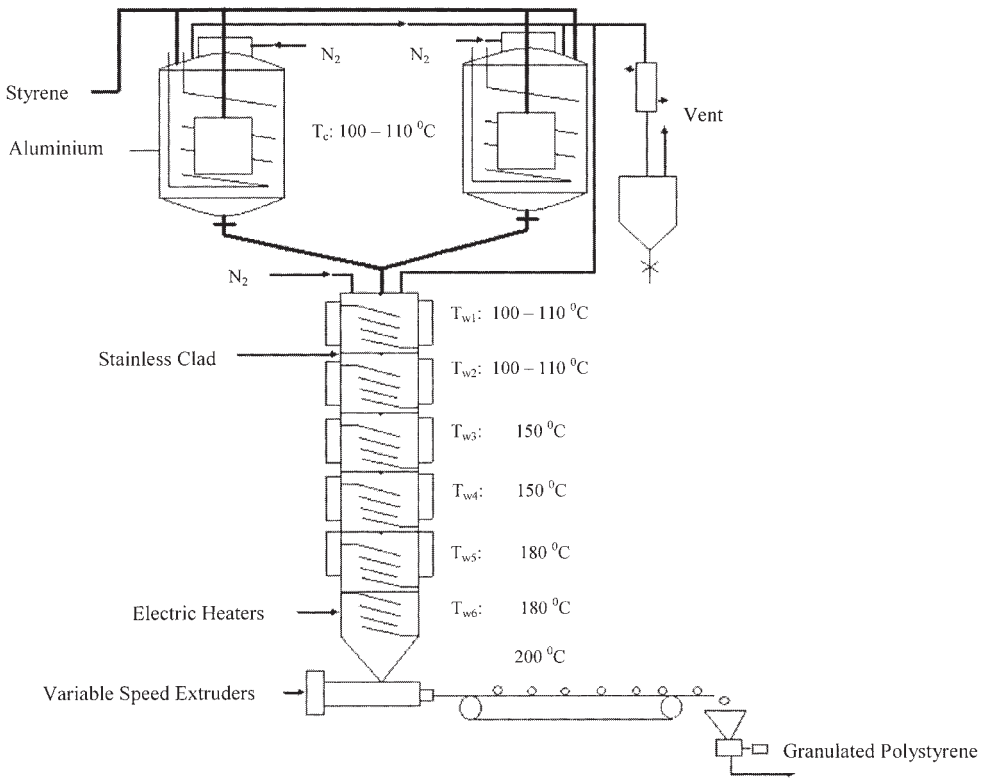

Figure 1 Schematic of the continuous tower process.[21]

quence of a CSTR and a tubular reactor) in the tower process, are then written. These are given in Table III. Our model accounts for the density change taking place in these reactors assuming the additivity of volumes. Our model differs slightly from that used by Hui and Hamielec[7] and Pryor and Coco.[21] These workers invoked the quasi-steady-state hypothesis, but we have not done so. The gel effect is very prominent in the polymerization of styrene and, because chain initiation remains essentially unaffected by it, hindered termination must cause the accumulation of intermediate radicals in the reaction mass, making the quasi-steady-state hypothesis a poor approximation.

The balance equations for the CSTR (at T_c) constitute a set of nine coupled nonlinear algebraic equations. The numerical methods for solving such equations require estimating values for each of the dependent variables. We solved these equations using the technique described in Table IV and found that it converged all the time.

TABLE II
Temperatures Used in the Tower Process and the Corresponding Reaction Characteristics

Decision variable	Industrial value (K)[20]	Simulation value (K)	Optimal chromosome (K)	
			Set 1	Set 2
T_c	353–355	354	353.59	353.85
T_{w1}	373–383	378	376.68	377.41
T_{w2}	373–383	378	382.52	382.95
T_{w3}	423	423	434.29	434.64
T_{w4}	423	423	437.90	408.61
T_{w5}	453	453	448.10	457.59
T_{w6}	453	453	447.70	456.30
x_c	—	0.3317	0.3228	0.3285
x_f	—	0.9948	0.9953	0.9950
PDI_f	—	3.2950	3.3346	3.3147
10^{-5} M_{Nf}, kg/kmol	1.870	1.8700	1.8700	1.8700

TABLE III
Model Equations for the Tower Process

CSTR (assuming pure monomer feed)

$$M = M_0 - \frac{V_c}{Q^2}(k_p M \lambda_0)$$

$$R_1 = \frac{V_c}{Q^2}\left[\frac{2k_i M^3}{Q} - k_p R_1 M - k_t R_1 \lambda_0 + k_{fm} M(\lambda_0 - R_1)\right]$$

$$\lambda_0 = \frac{V_c}{Q^2}\left(\frac{2k_i M^3}{Q} - k_t \lambda_0^2\right)$$

$$\lambda_1 = \frac{V_c}{Q^2}\left[\frac{2k_i M^3}{Q} + k_p M \lambda_0 + k_{fm} M \lambda_0 - (k_t \lambda_0 \lambda_1 + k_{fm} M \lambda_1)\right]$$

$$\lambda_2 = \frac{V_c}{Q^2}\left[\frac{2k_i M^3}{Q} + 2k_p \lambda_1 M + k_p M \lambda_0 + k_{fm} M \lambda_0 - (k_t \lambda_0 \lambda_2 + k_{fm} M \lambda_2)\right]$$

$$\mu_0 = \frac{V_c}{Q^2}\left[\frac{k_t}{2}\lambda_0^2 + k_{fm} M(\lambda_0 - R_1)\right]$$

$$\mu_1 = \frac{V_c}{Q^2}[k_t \lambda_1 \lambda_0 + k_{fm} M(\lambda_1 - R_1)]$$

$$\mu_2 = \frac{V_c}{Q^2}[k_t(\lambda_0 \lambda_2 + \lambda_1^2) + k_{fm} M(\lambda_2 - R_1)]$$

$$Q = W_M\left[\frac{M}{\rho_M} + \frac{(M_0 - M)}{\rho_P}\right]$$

$$x \equiv 1 - \frac{M}{M_0}$$

Nonisothermal PFR

$$\frac{dM}{dz} = -\frac{A_c}{Q^2}(k_p M \lambda_0)$$

$$\frac{dR_1}{dz} = \frac{A_c}{Q^2}\left[\frac{2k_i M^3}{Q} - k_p R_1 M - k_t R_1 \lambda_0 + k_{fm} M(\lambda_0 - R_1)\right]$$

$$\frac{d\lambda_0}{dz} = \frac{A_c}{Q^2}\left(\frac{2k_i M^3}{Q} - k_t \lambda_0^2\right)$$

$$\frac{d\lambda_1}{dz} = \frac{A_c}{Q^2}\left[\frac{2k_i M^3}{Q} + k_p M \lambda_0 + k_{fm} M \lambda_0 - (k_t \lambda_0 \lambda_1 + k_{fm} M \lambda_1)\right]$$

$$\frac{d\lambda_2}{dz} = \frac{A_c}{Q^2}\left[\frac{2k_i M^3}{Q} + 2k_p \lambda_1 M + k_p M \lambda_0 + k_{fm} M \lambda_0 - (k_t \lambda_0 \lambda_2 + k_{fm} M \lambda_2)\right]$$

$$\frac{d\mu_0}{dz} = \frac{A_c}{Q^2}\left[\frac{k_t}{2}\lambda_0^2 + k_{fm} M(\lambda_0 - R_1)\right]$$

$$\frac{d\mu_1}{dz} = \frac{A_c}{Q^2}[k_t \lambda_1 \lambda_0 + k_{fm} M(\lambda_1 - R_1)]$$

$$\frac{d\mu_2}{dz} = \frac{A_c}{Q^2}[k_t(\lambda_0 \lambda_2 + \lambda_1^2) + k_{fm} M(\lambda_2 - R_1)]$$

$$\frac{dT}{dz} = \frac{1}{\rho_0 v_0 c_p}\left[-\Delta H\left(\frac{k_p M \lambda_0}{Q^2}\right) - \frac{(UL)}{\pi r^2}(T - T_w)\right]$$

$$Q = W_M\left[\frac{M}{\rho_M} + \frac{(M_0 - M)}{\rho_P}\right]$$

$$x \equiv 1 - \frac{M}{M_0}$$

$$\frac{(UL)}{(UL)_{c,\text{ref}}} = \left(\frac{x_{c,\text{ref}}}{x}\right)^{0.893}\left(\frac{M_{Wc,\text{ref}}}{M_W}\right)^{0.19\beta}\exp\left\{218.5\left[\frac{\exp(2.4x_{c,\text{ref}})}{T_{c,\text{ref}}} - \frac{\exp(2.4x)}{T}\right]\right\}$$

$\beta = 1$ if $M_W \leq 40{,}000/x$
$\beta = 3.4$ if $M_W > 40{,}000/x$
at $z = 0$: use the combined values from the two CSTRs

TABLE IV
Procedure Used for Simulating the CSTR

In the equations for M and λ_0 for the CSTR (Table III), λ_0 can be eliminated to give

$$\frac{2k_t(M_0 - M)}{k_pM} - \sqrt{1 + \frac{8V_c^2k_tk_iM^3}{Q^5}} + 1 = 0 \tag{IVa}$$

where M_0 is the feed flow rate to a single CSTR.

Using the rate expressions for k_t (in terms of x, because of the Trommsdorff effect; Table V) and using the expression for x in terms of M in the above equation, we obtain the following equation for M:

$$\frac{2k_{t0}\exp\left\{-2\left[A_1\left(1-\frac{M}{M_0}\right)+A_2\left(1-\frac{M}{M_0}\right)^2+A_3\left(1-\frac{M}{M_0}\right)^3\right]\right\}(M_0-M)}{k_pM} - \sqrt{1+\frac{8V_c^2k_tk_{t0}\exp\left\{-2\left[A_1\left(1-\frac{M}{M_0}\right)+A_2\left(1-\frac{M}{M_0}\right)^2+A_3\left(1-\frac{M}{M_0}\right)^3\right]\right\}M^3}{Q^5}} + 1 = 0 \tag{IVb}$$

where

$$Q = W_M\left[\frac{M}{\rho_M} + \frac{(M_0 - M)}{\rho_P}\right] \tag{IVc}$$

In this equation, Q is the volumetric flow rate at the exit of the CSTR, a function of M. We solve eqs. (IVb) and (IVc) using the NAG library subroutine C05ADF to obtain the converged values of M. This code uses the Bus and Dekker algorithm [for finding the zeros of a function within a range (EPS), specified by the user]. The value of EPS used was 10^{-5}, and the range of M specified was $M \in [5.93 \times 10^{-3}, 5.93 \times 10^{-2}]$. The other flows and moments at the exit of the CSTR can be calculated in the sequence: λ_0, R_1, λ_1, λ_2, μ_0, μ_1, and μ_2, using the corresponding equations (the exact expressions can be supplied on request).

The tubular reactor is modeled assuming it to be a plug flow reactor (PFR). Use of the diffusion terms is not necessary in view of the observations of Wallis et al.[9] The exothermic nature of this reaction causes the temperature to vary along the length of the reactor (no radial gradients are assumed to be present). Thus, in addition to the mass balance and moment equations, an energy balance equation is required. Our model for this reactor thus consists of nine coupled ordinary differential equations–initial value problem (ODE–IVPs), which are integrated using Gear's technique[37] (code D02EJF in the NAG library; with TOL = 10^{-15}).

The energy balance equation requires the modeling of the heat transfer from the reaction mass to the cooling liquid, both in the external jacket and in the internal cooling coils (both at[20] T_{wi}). This term is given by $U(Ldz)(T - T_{wi})$, where Ldz is the total heat transfer area in the length dz. Clearly, L is some kind of an equivalent length for heat transfer. Boundy and Boyer[38] mention that the six sections in the tower have similar geometries (although the detailed geometry is not provided), and so L is the same in all six sections of the PFR. It is difficult to estimate the overall heat transfer coefficient U, and we do not know the exact value of L. Hence, in the heat balance equation, we consider the combination UL, together, and attempt to estimate this. We assume that most of the heat is transferred from/to the cooling coils and that the contribution of the jacket-side heat transfer is negligible. In such a case, U is determined solely by the flow pattern inside the PFR. The reaction mass flows across a series of helical tubes, which can be approximated as the flow past a bank of tubes for which we can write[39]

$$U \propto (\mathrm{Re})^{0.52}(\mathrm{Pr})^{0.33} \tag{1}$$

The Reynolds (Re) and Prandtl (Pr) numbers depend on the density ρ, the viscosity μ, the specific heat c_p, and the thermal conductivity k of the reaction mass. All of these change as the reaction mass travels downstream. Of these, the change of μ (with the monomer conversion x and the weight-average molecular weight M_W) is expected to be the most significant. We assume, therefore, that the variation in U along the length of the reactor is solely associated with the variation in μ. The following dependency of μ on the properties of the reaction mixture is used[40]:

$$\mu \propto (x)^{4.7}(M_W)^{\beta}\exp\left[\frac{2300\exp(2.4x)}{\mathrm{RT}}\right] \tag{2}$$

where

TABLE V
Values Used for Simulation[7,9,20]

Parameters and properties/details of the tower process	Reference
Parameters	
$\rho_M = 924 - 0.918(T - 273.1)$, kg/m^3	7
$\rho_P = 1084.8 - 0.605(T - 273.1)$, kg/m^3	7
$k_i = 2.19 \times 10^{-1} \exp\left(-\frac{13810}{T}\right)$, m^6 mol^{-2} s^{-1}	7
$k_p = 1.051 \times 10^4 \exp\left(-\frac{3557}{T}\right)$, m^3 mol^{-1} s^{-1}	7
$k_{fm} = k_{fm\,0} - Bk_p x$	7
$k_{fm0} = 2.31 \times 10^3 \exp\left(-\frac{6377}{T}\right)$, m^3 mol^{-1} s^{-1}	7
$B = 1.013 \times 10^{-3} \log_{10}\left(\frac{473.12 - T}{202.5}\right)$	7
$k_t = k_{t0} \exp[-2(A_1 x + A_2 x^2 + A_3 x^3)]$, m^3 mol^{-1} s^{-1}	7
$k_{t0} = 1.225 \times 10^6 \exp\left(-\frac{844}{T}\right)$, m^3 mol^{-1} s^{-1}	7
$A_1 = 2.57 - 5.05 \times 10^{-3} T$	7
$A_2 = 9.56 - 1.76 \times 10^{-2} T$	7
$A_3 = -3.03 + 7.85 \times 10^{-3} T$	7
$W_M = 0.10414$ kg/mol	—
$c_p = 107.66$ J kg^{-1} K^{-1}	9
$\Delta H = -4000$ J/mol	9
$(UL)_{c,\mathrm{ref}} = 47.88$ W m^{-1} K^{-1}	This work
$T_{c,\mathrm{ref}} = 354$ K	This work
$x_{c,\mathrm{ref}} = 0.3317$	This work
$M_{Wc,\mathrm{ref}} = 1.083 \times 10^6$ kg/kmol	This work
Details of the reactor and process	
$M_0^* = 1.186 \times 10^{-1}$ mol/s	20
$V_c = 1.370$ m^3	20
$L_T = 6$ m	20
$r = 0.375$ m	20

$$\beta = 1 \quad \text{if } M_W \le 40{,}000/x$$

$$\beta = 3.4 \quad \text{if } M_W > 40{,}000/x \tag{3}$$

The following dependency of U on the polymer properties can be deduced from eqs. (1)–(3):

$$U \propto \frac{1}{x^{0.893} M_W^{0.19\beta} \exp\left[\frac{218.5 \exp(2.4x)}{T}\right]} \tag{4}$$

The value of UL at the beginning of the PFR (exit of the CSTR) for the industrial reactor under current (industrial) operating conditions (Table II, column 3; Table V) is taken as a tuning parameter $(UL)_{c,\mathrm{ref}}$. The value of (UL) at any axial position z along the PFR under any set of operating conditions can then be written as

$$\frac{(UL)}{(UL)_{c,\mathrm{ref}}} = \left(\frac{x_{c,\mathrm{ref}}}{x}\right)^{0.893} \left(\frac{M_{Wc,\mathrm{ref}}}{M_W}\right)^{0.19\beta} \times \exp\left\{218.5\left[\frac{\exp(2.4x_{c,\mathrm{ref}})}{T_{c,\mathrm{ref}}} - \frac{\exp(2.4x)}{T}\right]\right\} \tag{5}$$

In eq. (5), $x_{c,\mathrm{ref}}$ and $M_{Wc,\mathrm{ref}}$ are the computed values at the end of the CSTR for the current (industrial) case, and $T_{c,\mathrm{ref}}$ is the corresponding temperature of the CSTR (=354 K). The values of $x_{c,\mathrm{ref}}$ and $M_{Wc,\mathrm{ref}}$ are 0.3317 and 1,083,000 kg/kmol, respectively. We treat $(UL)_{c,\mathrm{ref}}$ as the sole tuning parameter and solve the model equations using the parameters for the industrial unit[7,9,20] (as given in Table V, and using the temperatures as given in Table II, column 3) until the exit value of the number-average molecular weight M_N, predicted by our code, matches the industrial value[20] of 187,000 kg/kmol. This match was achieved with $(UL)_{c,\mathrm{ref}} = 47.88$ W m^{-1} K^{-1}. The reference values of the three parameters thus determined are used for all other operating conditions as well, when needed for obtaining the optimal conditions.

Optimization

The tuned model was then used with an optimization code for NSGA-II[22,23] to obtain improved (optimal) operating conditions for the tower process. An important objective function would be to minimize the unconverted monomer content in the final polymer because this can oligomerize readily,[19,38] rendering the polymer unstable, or react with other compounds in the environment to form undesirable products. In addition, minimization of the unreacted monomer in the product economizes the downstream processing units for its removal. Thus one objective function is to maximize the final (f) conversion x_f of styrene in the product. At the same time it is essential to maintain the molecular homogeneity of the product. This is quantified in terms of the polydispersity index (PDI): the lower the PDI, the better is the product in terms of its properties. Thus our second objective function aims at minimizing PDI_f, the PDI of the product. We thus optimize the following two objectives:

$$\max I_1(\mathbf{u}) \equiv x_f \tag{6a}$$

$$\min I_2(\mathbf{u}) \equiv \mathrm{PDI}_f \tag{6b}$$

The formulation of the optimization problem, in terms of two objective functions at the beginning itself, ensures its generality. If the two selected objective functions happen to be nonconflicting, we will obtain a unique solution (rather than a Pareto set of nondominated solutions) automatically. The control vector $\mathbf{u}$ is composed of T_c and T_{wi} $(i = 1, 2, \ldots, 6)$. These will

have some lower and upper bounds specified, based on operational reasons.

In addition to defining the objective functions, we need to add some end-point constraints. One important constraint is to ensure that the product has a design value (M_{Nd} = 187,000) of M_N, that is,

$$M_{Nf} = M_{Nd} \tag{7}$$

It is well known that the reaction mass becomes extremely viscous as the conversion increases. It becomes very difficult to ensure proper mixing and effective dissipation of heat in a CSTR above a monomer conversion of about 35%.[20] We thus limited the range of x_c, the conversion in the CSTR, to between 30 and 36%. This requirement can be written in the form of two inequality constraints

$$x_c \geq 0.30 \tag{8a}$$

$$x_c \leq 0.36 \tag{8b}$$

The solution of the above problem would suggest improvements in the operating conditions of the industrial process, if this is possible.

The optimization code for NSGA-II, available to us, maximizes both of the objective functions. Thus we need to transform our problem into one in which all the objectives are to be maximized. We do this by maximizing all the fitness functions,[41] F_i, defined as

$$\max I_1 \rightarrow \max F_1[\equiv I_1] \tag{9a}$$

$$\min I_2 \rightarrow \max F_2\left[\equiv \frac{1}{1+I_2}\right] \tag{9b}$$

The constraints on the molecular weight and the conversion [eqs. (7) and (8)] are usually taken care of by adding appropriate penalties[41] to the fitness functions. The resulting modified fitness functions that need to be maximized are given below, along with the other requirements:

$$\max F_1^*(\mathbf{u}) \equiv x_f - w_1\left(1 - \frac{M_{Nf}}{187{,}000}\right)^2 - w_2\{(\min[0, g_1])^2 + (\min[0, g_2])^2\} \tag{10a}$$

$$\max F_2^*(\mathbf{u}) \equiv [1/(1 + \mathrm{PDI}_f)] - w_1\left(1 - \frac{M_{Nf}}{187{,}000}\right)^2 - w_2\{(\min[0, g_1])^2 + (\min[0, g_2])^2\} \tag{10b}$$

subject to

$$\text{model equations} \tag{10c}$$

$$\mathbf{u}_{\min} \leq \mathbf{u} \leq \mathbf{u}_{\max} \tag{10d}$$

In eq. (10), the penalty terms g_1 and g_2 are defined as

$$g_1 \equiv 1 - \frac{x_c}{0.30} \tag{11a}$$

$$g_2 \equiv 1 - \frac{0.36}{x_c} \tag{11b}$$

In eq. (10), w_1 and w_2 are weighting factors for the penalties[41]; $\mathbf{u}_{\min}$ and $\mathbf{u}_{\max}$ refer to the lower and upper bounds on the set of decision variables $\mathbf{u}$, respectively; and min[0, g_1] and min[0, g_2] are bracketed penalties[22,41] defined as

$$\min[0, g] = \begin{bmatrix} 0, & \text{if } g \leq 0 \\ g, & \text{otherwise} \end{bmatrix} \tag{12}$$

Clearly, use of the two g functions adds on a penalty term to the modified objectives, F_i^*, when the inequalities in eq. (8) are violated.

Several (standard[25,27]) checks were made to ensure that our results were, indeed, optimal and correct. These are not discussed here but are similar to those used in our earlier work.[43,45] The CPU time taken on an Intel Pentium 4, with 1.7-GHz processor (Intel, Santa Clara, CA) and 256 MB RAM for one full optimization run (300 generations) was 42 min.

RESULTS AND DISCUSSION

A computer code was first written (in Fortran 90) and solved to integrate the model equations (ODE–IVPs) for the polymerization reaction in an isothermal batch reactor. The equations for this reactor can easily be written[42] using those for the PFR in Table III [by replacing the premultiplier A_c/Q^2 on the right-hand side of the several equations by $1/V$, where V is the volume of the reaction mass in the batch reactor at time t. The multiplier $1/Q$ in several terms on the right in Table III also needs to be replaced by $1/V$. M, R_1, λ_i, and μ_i are the total moles and moments for a batch reactor. The volume V of the reaction mass is given by the right-hand side of the equation for Q in Table III]. This code was run for three different (constant) temperatures, 100, 140, and 170°C, for predicting the monomer conversions and molecular weights at different instants of time t. The results were found to be in close agreement with the experimental values reported by Hui and Hamielec.[7] These simulation runs served to establish the validity of our model and our code (for batch reactors) over wide ranges of temperature (100–200°C) and conversion (0–99.5%). The code was then modified to predict the monomer conversion, the number- and weight-average molecular

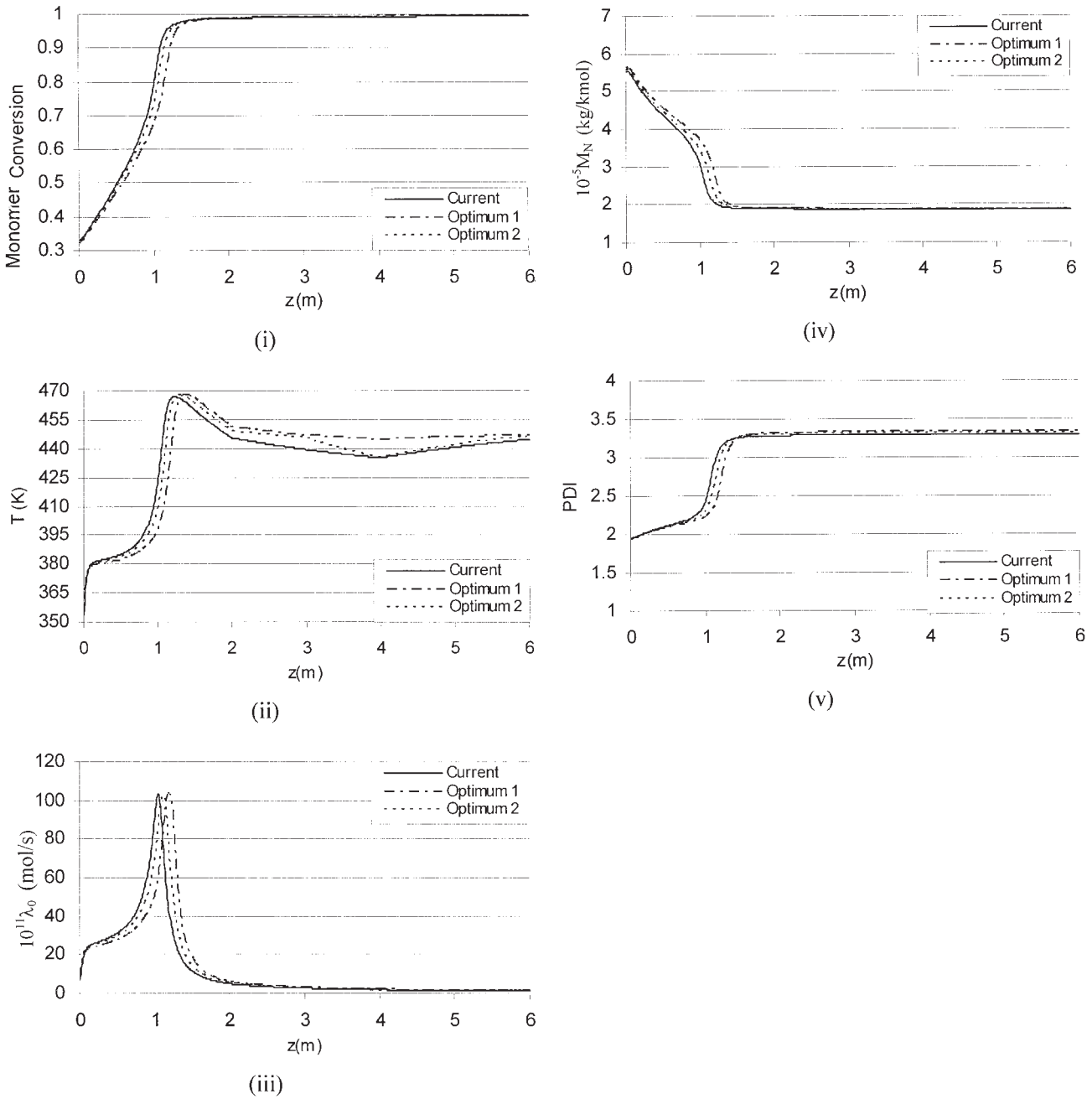

Figure 2 Results corresponding to the industrial reactor under current operating conditions (Table II, column 3), and under two optimal conditions (Table II, columns 4 and 5).

weights, and the PDI of the polymer, at the exit of the CSTR (input of the PFR: $z = 0$) as well as at any axial location z in the PFR. The temperature (T) of the reaction mixture was also computed in the PFR as a function of z. In all these cases, T_c and T_{wi} ($i = 1, 2, \ldots, 6$) were used as input parameters (operating conditions). The CSTR alone was simulated at $T_c = 80°C$. About 31.5% monomer conversion (at a rate of polymerization of 0.487% monomer conversion/h) was observed, which is very close to the value reported by Henderson and Bouton.[19]

The variables and parameters associated with the industrial tower process are specified in Table V and the temperatures used are given in Table II, column 3. Columns 4 and 5 in Table II correspond to two sets of optimal conditions (defined later in this article) for this reactor system. Figure 2 shows some results for these three cases. This figure shows that most of the monomer conversion takes place in the CSTR and the first two sections of the PFR. The remaining sections of the PFR are required primarily for "finishing" [i.e., attaining very high values ($\sim$ 99.5%) of the monomer con-

TABLE VI
Details of the Tower Process Under Two Sets of Optimal Conditions

End of section	T (K)	x	$10^{-5}M_N$	PDI
		Set 1[a]		
CSTR	353.59	0.3227	5.631	1.950
1	397.61	0.6716	3.670	2.226
2	450.95	0.9873	1.891	3.318
3	446.68	0.9918	1.878	3.328
4	444.45	0.9935	1.874	3.331
5	445.88	0.9945	1.871	3.333
6	446.65	0.9953	1.870	3.335
		Set 2[b]		
CSTR	353.85	0.3285	5.580	1.952
1	408.86	0.7261	3.378	2.303
2	448.85	0.9878	1.887	3.302
3	445.34	0.9918	1.877	3.310
4	434.92	0.9933	1.874	3.312
5	441.73	0.9942	1.872	3.313
6	446.37	0.9950	1.870	3.315

[a] Table II, column 4.
[b] Table II, column 5.

version x]. The temperature of the reaction mass starts to increase dramatically in the first section of the PFR, attains a maximum somewhere at the beginning of the second section, and then begins to decrease in the second section itself. This decrease is brought about by the combined effect of lower heat generation (associated with decreasing rates of polymerization) and larger heat transfer to the cooling fluid (attributed to the large temperature difference). The temperature continues to decrease until the fourth section of the PFR, after which the high wall temperatures cause an increase in T (primarily, a heat-transfer effect). The radical concentration rises steeply in the first section of the PFR because of high temperatures, then falls and stabilizes at a low value. The presence of radicals in large concentrations causes a reduction in the number-average molecular weight M_N; thus M_N decreases along the length of the PFR, with most of this occurring in the first two sections. Table VI shows that sections 3–6 of the PFR help to achieve slightly higher conversions (finishing), a slow process, without affecting the average molecular weights much. Higher temperatures in these sections would speed up the reaction, but at the cost of lower molecular weights and, possibly, some degradation of the product (in fact, we do not allow the temperature of the reaction mass anywhere in the PFR to go above 200°C for this reason, and because our rate equations fail thereafter).

Simulation results were also generated for several other sets of operating conditions. These results are not provided here (but can be supplied on request). Based on simulations with several other sets of operating conditions, we found that the temperature of the CSTR and the wall temperatures of the first two sections determine whether thermal runaway would occur at any point in the tower. The wall temperatures of the last four sections play a very small role in determining thermal runaways.

Having gained some insight into the continuous tower process, through our simulation studies, we turned our attention to its optimization [described in eq. (10)] to see whether the current set of operating conditions (for the specified reactor) is, indeed, the best. The computational parameters used for optimization are given in Table VII. The bounds for the decision variables are taken to encompass the operating conditions used currently in industry.[20] During optimization, all the solutions in which the temperature goes beyond 200°C are killed by assigning a large penalty.

Figure 3 shows the evolution of the solutions (parent population) over the generations. All N_p (=100) solutions are shown. In the early generations, several of these solutions do not satisfy the constraints [eqs. (7) and (8)]. Figure 4 shows the hundred solutions in the fifth generation. All of these are found to satisfy the constraint $0.30 \leq x_c \leq 0.36$. However, 21 chromosomes are found to lie just outside a small range, $186{,}000 \leq M_{Nf} \leq 188{,}000$, less than 1% around the desired value of 187,000. These 21 chromosomes are shown as unfilled diamonds in Figure 4. It is clear from Figure 4(iii) that several solutions exist that satisfy both the constraints within the bounds mentioned above, and that some of these are better than others. It is clear that an optimal solution(s) exists. As the generations proceed, newer solutions are also generated, finally giving a set of optimal solutions [Fig. 3(vi)].

It is observed that, at the 300th generation, we obtain essentially two optimal solutions. These are repeated several times. The details of these two optimal points are provided in Table II, columns 4 and 5. The

TABLE VII
NSGA Parameters Used for Optimization[22,41]

Control variable	Lower bound (K)	Upper bound (K)
T_c	353	358
T_{w1}	370	380
T_{w2}	376	383
T_{w3}	408	438
T_{w4}	408	438
T_{w5}	438	463
T_{w6}	438	463

$N_p = 100$
$N_{str} = 16$
$p_c = 0.85$
$p_m = 0.01$
$w_1 = w_2 = 10^8$
Random seed = 0.88876
$N_{g,\max} = 300$

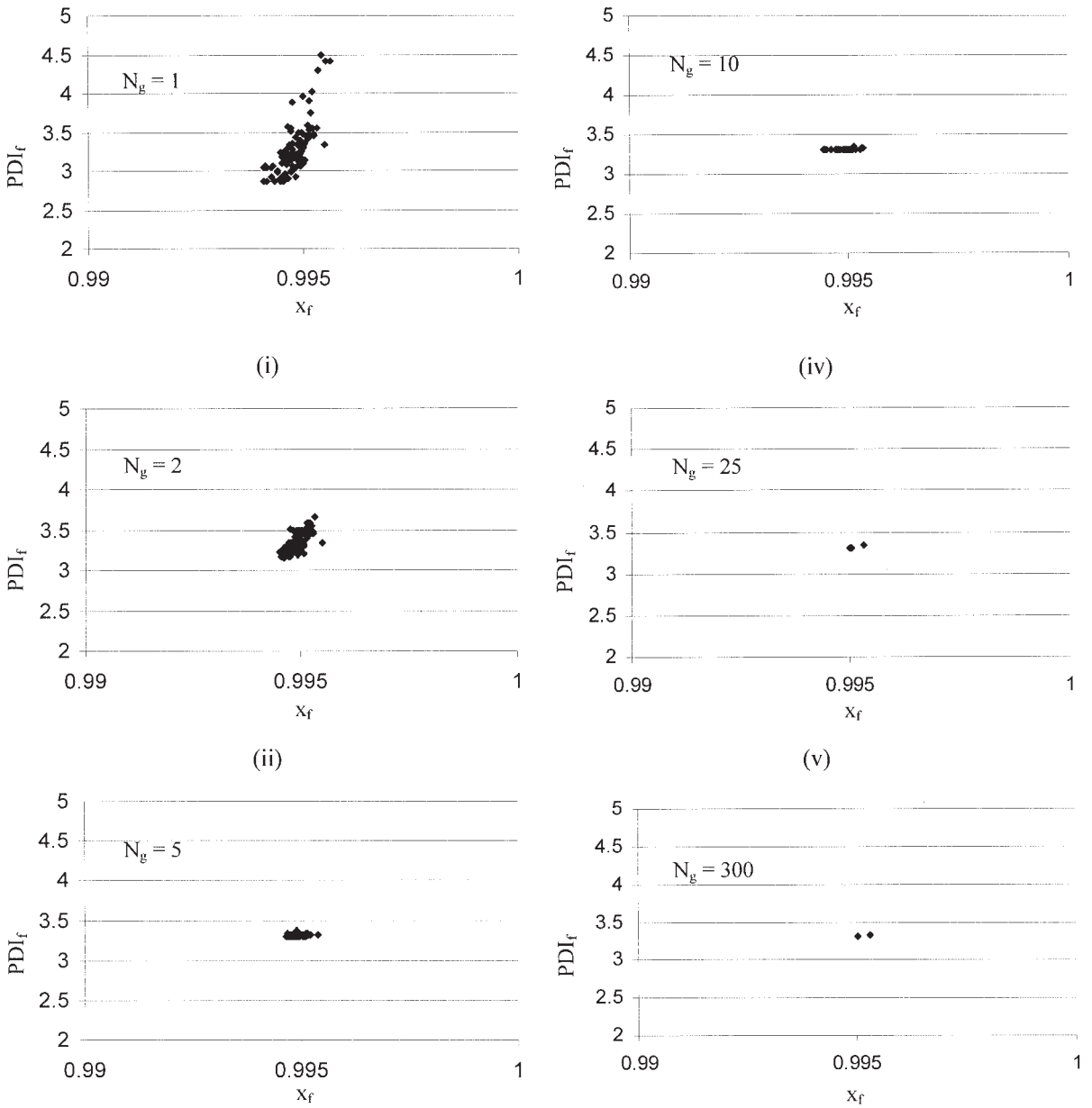

Figure 3 Evolution of the chromosomes over the generations.

constraint on M_{Nf} is satisfied almost exactly for these two solutions. Because the values of x_f and PDI_f for these two are quite close, we can consider that we have a unique solution (with a minor amount of scatter). Such scatter has been observed in several of our earlier optimization studies of industrial relevance.[24] The values of the seven decision variables, corresponding to the optimal chromosomes, are also shown in Figure 3, along with the values used currently. A single objective optimization problem was solved, using the function F_1^* (involving the monomer conversion x_f, in the presence of a constraint on M_{Nf}), alone with the same constraints and bounds as in the two-objective problem; this gave the same (unique) solution. Similar qualitative results were previously obtained for methyl methacrylate polymerization.[43] This is not surprising, given that both polystyrene and poly methyl methacrylate follow similar kinetics (free-radical polymerization in the presence of the Trommsdorff effect). This suggests that the two objectives used in the present study are not conflicting, and that the optimization is influenced primarily by the equality constraint on M_N and not by the PDI. However, in a complex system such as this, one cannot guess, *a priori*, whether this would be the case, and one is forced to solve the more general, two-objective function problem.

The optimal values of the decision variables are compared with the industrial values in Table II (columns 3, 4, and 5). It is observed that the optimal

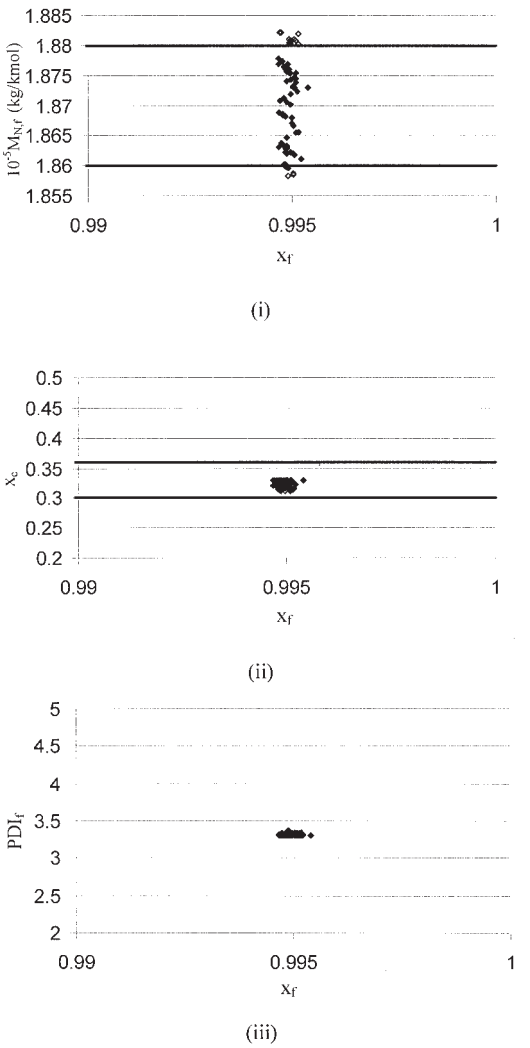

Figure 4 M_{Nf}, x_c, and PDI_f for all 100 chromosomes as a function of x_f, in the fifth generation. Chromosomes violating the constraint, $186{,}000 \leq M_{Nf} \leq 188{,}000$, are shown as unfilled diamonds. All other chromosomes are shown as filled diamonds (these superpose over the unfilled diamonds in ii and iii).

values of T_c and T_{w1} are almost the same as those currently used in industry. The value of T_{w2} is about 4°C higher. The optimal values of T_{w3}, T_{w4}, T_{w5}, and T_{w6}, however, are a bit different. It is found that the use of the optimal temperature profile leads to a slightly higher value of x_f compared to the current (simulated) value in the industrial reactor, but the PDI_f is higher. However, these deviations are insignificant, practically speaking, and it can be inferred that the continuous tower process is running under near-optimal operating conditions.

Because NSGA-II involves several computational parameters, it is very important to analyze how the final results are affected by the variations in these parameters. The three most important parameters are the crossover probability p_c, the mutation probability p_m, and the seed for the generation of random numbers. The dependency of the optimal solutions on these computational parameters is shown in Figure 6. These results show as much scatter as the converged final results in Figure 5. The two constraints [eqs. (7) and (8)] are found to be satisfied (almost exactly for M_{Nf}).

CONCLUSIONS

The popular tower process for the production of polystyrene was simulated and optimized. A unique optimal point was obtained when we used two objective functions, reflecting the fact that the two objectives are nonconflicting in nature. Interestingly, this optimal solution lies quite close to the industrial values.

NOMENCLATURE

Symbol

Abbreviation Description

A	Styryl radical
A_c	Area of cross section of the PFR, m^2
AH	Diels–Alder adduct
c_p	Specific heat of the reaction mixture, J kg^{-1} K^{-1}
D	Outside diameter of cooling coil, m
ΔH	Heat of reaction, J/mol
K	Thermal conductivity of the reaction mass, W m^{-1} K^{-1}
k_{fm0}	Rate constant for chain transfer at zero conversion of styrene, m^3 mol^{-1} s^{-1}
k_{fm}	Actual rate constant for chain transfer, m^3 mol^{-1} s^{-1}
k_i	Rate constant for initiation, m^6 mol^{-2} s^{-1}
k_p	Rate constant for propagation, m^3 mol^{-1} s^{-1}
k_{t0}	Rate constant for termination at zero conversion of styrene, m^3 mol^{-1} s^{-1}
k_t	Actual rate constant for termination, m^3 mol^{-1} s^{-1}
L	Equivalent length for heat transfer in the PFR ($Ldz \equiv$ heat transfer area in dz)
L_T	Actual total length of the PFR, m
M	Molar flow rate of styrene in the CSTR at the outlet, and at any z in the PFR, mol/s
M_N	Number-average molecular weight of polystyrene $\{[(\lambda_1 + \mu_1)/(\lambda_0 + \mu_0)]W_M\}$, kg/kmol
M_0	Molar flow rate of monomer feed to a single CSTR, mol/s
M_0^*	Molar flow rate of monomer feed to the tower process ($=2M_0$), mol/s
M_W	Weight-average molecular weight of polystyrene $\{[(\lambda_2 + \mu_2)/(\lambda_1 + \mu_1)]W_M\}$, kg/kmol
N_g	Generation number
N_p	Number of chromosomes in the population
N_{str}	Number of binary digits representing each control variable
p_c	Crossover probability

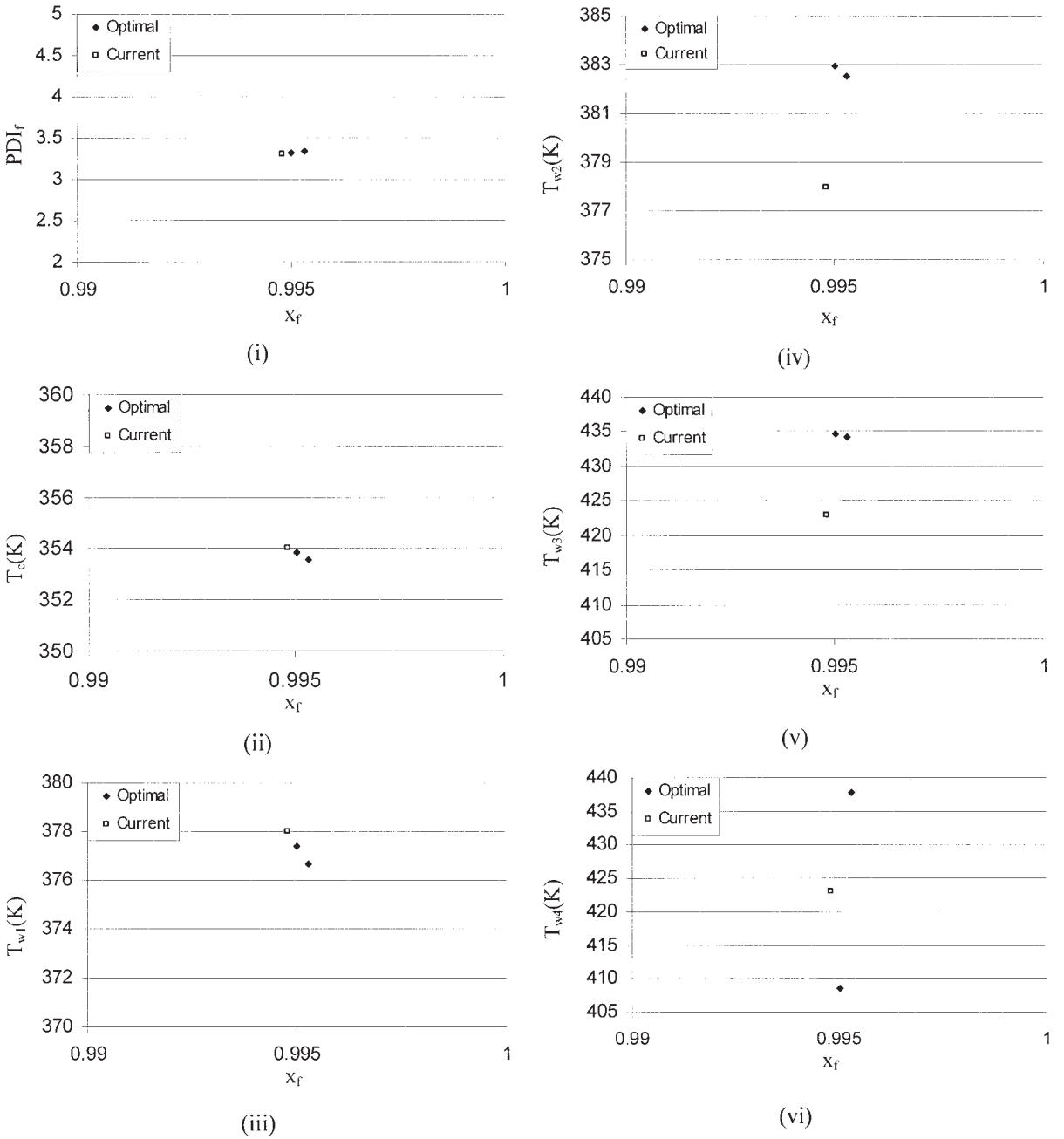

Figure 5 Optimal results of the reference run at the 300th generation.

p_m Mutation probability
PDI Polydispersity index (M_W/M_N)
P_r Dead polymer containing r monomeric units
Pr Prandtl number ($\equiv \mu c_p/K$)
Q Volumetric flow rate in the CSTR at the outlet, and at any z in the PFR, m^3/s
r Inner radius of the tubular reactor, m
R_r Polymer radical containing r monomer units
Re Reynolds Number ($\equiv D\rho v/\mu$)
S Styrene
t Reaction time in the batch reactor, s
T Temperature of the reaction mixture, K
T_w Wall temperature of the PFR, K
U Overall heat transfer coefficient, W m^{-2} K^{-1}
v Velocity of the reaction mass in the PFR, m/s
V_c Volume of a single CSTR, m^3
W_M Molecular weight of styrene, kg/mol
x Conversion of styrene
z Length along the axial direction in the PFR, m

Greek letters

β A parameter in the viscosity correlation

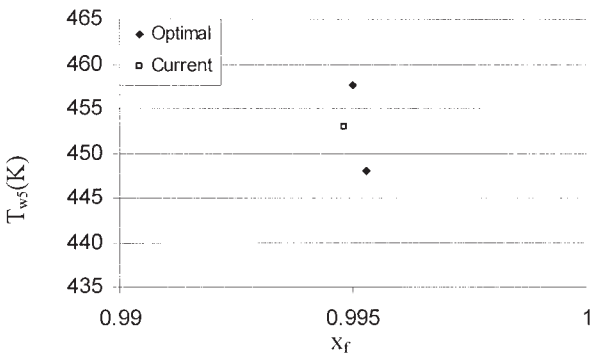

(vii)

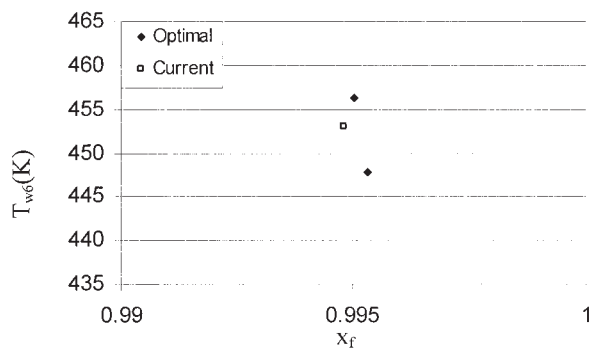

(viii)

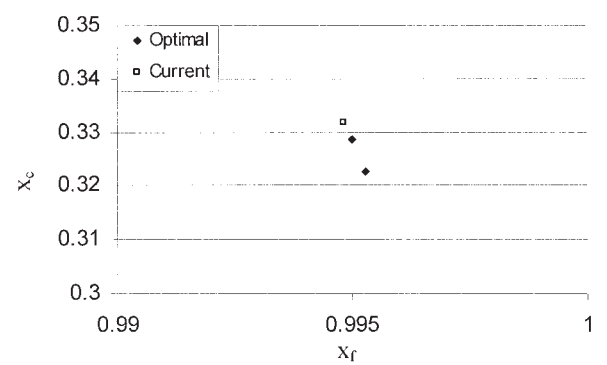

(ix)

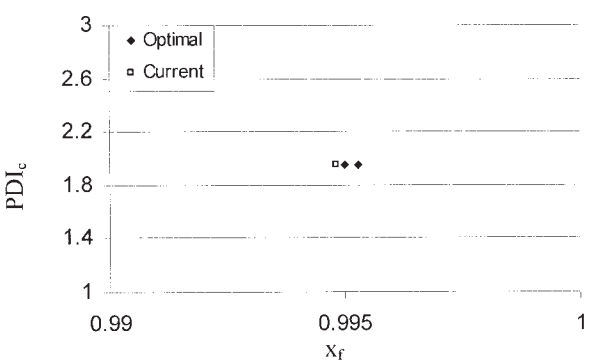

Figure 5 *(Continued from the previous page)*

λ_k kth moment of radicals ($\equiv\Sigma_{r=1}^{\infty} r^k R_r$); $k = 0, 1, 2, \cdots$; in the CSTR at the outlet, or at any z in the PFR, mol/s

μ Viscosity of the reaction mass, Pa s

μ_k kth moment of polymers ($\equiv\Sigma_{r=2}^{\infty} r^k P_r$); $k = 0, 1, 2, \cdots$; in the CSTR at the outlet, or at any z in the PFR, mol/s

ρ_M Density of styrene (kg/m^3); in the CSTR at the outlet, or at any z in the PFR

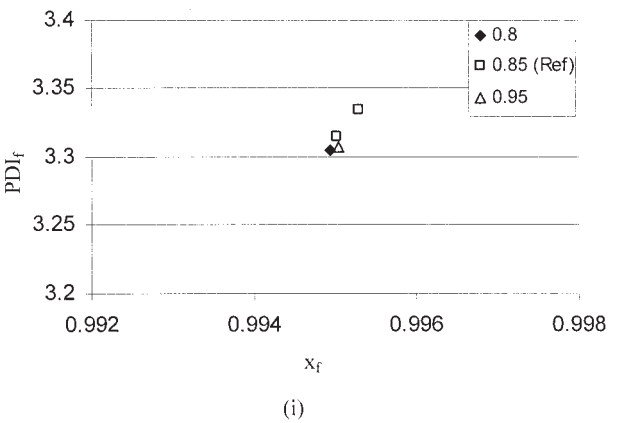

(i)

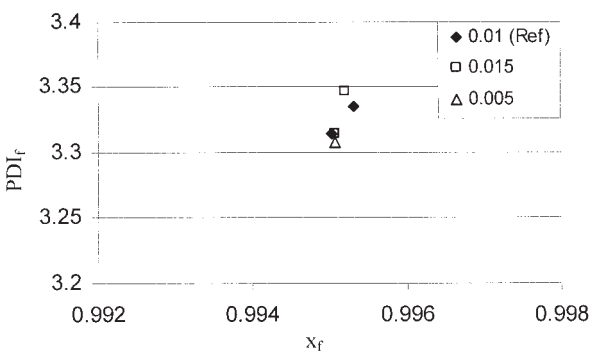

(ii)

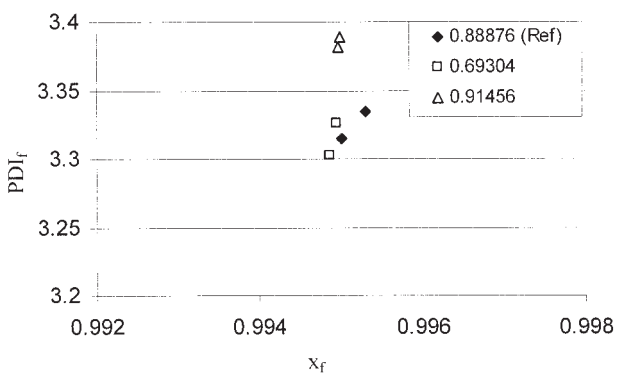

(iii)

Figure 6 Effect of computational parameters [(i) p_c; (ii) p_m; (iii) seed] on the optimal results. Reference values are p_c = 0.85, p_m = 0.01, seed = 0.88876. All chromosomes satisfy the two constraints exactly.

ρ_P Density of polystyrene (kg/m^3); in the CSTR at the outlet, or at any z in the PFR

Subscripts/superscripts

c CSTR (unless specified otherwise)
f Final; at the outlet of the PFR
i ith section in the PFR; $i = 1, 2, \ldots, 6$
w Wall
0 Inlet of the PFR (unless specified otherwise)
ref Reference value corresponding to the industrial case

Partial financial support from the Department of Science and Technology, Government of India, New Delhi [through Grant III-5(13)/2001-ET] is gratefully acknowledged.

References

1. Flory, P. J. J Am Chem Soc 1937, 59, 241.
2. Haward, R. N. Trans Faraday Soc 1950, 46, 204.
3. Zimm, B. J.; Bragg, J. K. J Polym Sci 1952, 9, 476.
4. Russell, K. E.; Tobolsky, A. V. J Am Chem Soc 1954, 76, 395.
5. Overberger, C. G.; Lapkin, M. J Am Chem Soc 1965, 77, 465.
6. Mayo, F. R. J Am Chem Soc 1968, 90, 1289.
7. Hui, A. W.; Hamielec, A. E. J Appl Polym Sci 1972, 16, 749.
8. Trommsdorff, V. E.; Kohle, H.; Lagally, P. Makromol Chem 1947, 1, 169.
9. Wallis, J. P. A.; Ritter, R. A.; Andre, H. AIChE J 1975, 21, 686.
10. Tadmor, Z.; Biesenberger, J. A. Ind Eng Chem Fundam 1966, 5, 336.
11. Gao, J.; Hungenberg, K. D.; Penlidis, A. Macromol Symp 2004, 206, 509.
12. Husain, A.; Hamielec, A. E. Continuous Polymerization Reactors; Bouton, T. C.; Chappelear, D. C., Eds.; AIChE Symposium Series; University of Delaware, Newark, DE, 1976; Vol. 72, p. 112.
13. I. G. Farbenindustrie. Ger. Pat. 634,278, 1936.
14. Smith, W. M. Manufacture of Plastics, Vol. I; Reinhold: New York, 1964.
15. Union Carbide U.S. Pat. 2,496,653, 1950.
16. Dow Chemical Co. U.S. Pat. 2,727,884, 1955.
17. Dow Chemical Co. U.S. Pat. 3,243,481, 1966.
18. Dow Chemical Co. U.S. Pat. 3,660,535, 1972.
19. Simon, R. H. M.; Chappelear, D. C. Polymerization Reactors and Processes; Henderson, J. N., Bouton, T. C., Eds.; ACS Symposium Series; American Chemical Society, Washington, D.C., 1979; p. 71.
20. Dunlop, R. D.; Reese, F. E. Ind Eng Chem 1948, 40, 654.
21. Pryor, W. A.; Coco, J. H. Macromolecules 1970, 3, 500.
22. Deb, K. Multiobjective Optimization Using Evolutionary Algorithms; Wiley: Chichester, UK, 2001.
23. Deb, K.; Pratap, A.; Agarwal, S.; Meyarivan, T. IEEE Trans Evol Comput 2002, 6, 182.
24. Bhaskar, V.; Gupta, S. K.; Ray, A. K. Rev Chem Eng 2000, 16, 1.
25. Kasat, R. B.; Kunzru, D.; Saraf, D. N.; Gupta, S. K. Ind Eng Chem Res 2002, 41, 4765.
26. Rajesh, J. K.; Gupta, S. K.; Rangaiah, G. P.; Ray, A. K. Ind Eng Chem Res 2000, 39, 706.
27. Nandasana, A. D.; Ray, A. K.; Gupta, S. K. Ind Eng Chem Res 2003, 42, 4028.
28. Inamdar, S. V.; Saraf, D. N.; Gupta, S. K. Chem Eng Res Dev 2004, 82A, 611.
29. Silva, C. M.; Biscaia, E. C., Jr. Comput Chem Eng 2003, 27, 1329.
30. Nayak, A.; Gupta, S. K. Macromol Theory Simul 2004, 13, 73.
31. Dantus, M. M.; High, K. A. Comput Chem Eng 1999, 23, 1493.
32. Oh, P. P.; Rangaiah, G. P.; Ray, A. K. Ind Eng Chem Res 2002, 41, 2248.
33. Ziyang, Z.; Hidajat, K.; Ray, A. K. Ind Eng Chem Res 2002, 41, 3213.
34. Yu, W.; Hidajat, K.; Ray, A. K. Ind Eng Chem Res 2003, 42, 6823.
35. Kasat, R. B.; Ray, A. K.; Gupta, S. K. Mater Manuf Process 2003, 18, 521.
36. Nandasana, A. D.; Ray, A. K.; Gupta, S. K. Int J Chem React Eng 2003, R2, 1.
37. Gupta, S. K. Numerical Methods for Engineers; New Age International: New Delhi, 1995.
38. Boundy, R. H.; Boyer, R. F. Styrene, Its Polymers, Copolymers and Derivatives; Reinhold: New York, 1952.
39. Holman, J. P. Heat Transfer, 8th ed.; McGraw-Hill: New York, 1997.
40. Biesenberger, J. A.; Sebastian, D. H. Principles of Polymerization Engineering; Wiley: New York, 1983.
41. Deb, K. Optimization for Engineering Design: Algorithms and Examples; Prentice Hall of India: New Delhi, 1995.
42. Wu, G. Z. A.; Denton, L. A.; Laurence, R. L. Polym Eng Sci 1982, 22, 1.
43. Garg, S.; Gupta, S. K. Macromol Theory Simul 1999, 8, 46.